EUGEN BOOS[1], MICHAEL SCHWARZENBERGER[1], MARTIN JARETZKI[2],
HAJO WIEMER[1], STEFFEN IHLENFELDT[1,2]

MELT POOL MONITORING USING FUZZY BASED ANOMALY DETECTION IN LASER BEAM MELTING

Abstract

With the introduction and further development of additive manufacturing (AM) processes and topology optimization algorithms, components are designed to meet high performance objectives. However, the quality standards required for the high-performance market are not entirely given yet. Known but hard to deterministically quantifiable influences have a considerable effect on the manufacturing process and consequently the microstructure and the mechanical properties of the components. Therefore, process monitoring systems are implemented for a better evaluation of the process itself and the quality of the component. Due to the challenging nature of the AM process, data uncertainties within the collected monitoring data are common. To achieve the high quality criteria not only an improved understanding of the present uncertain influences is crucial, but also correspondingly the correct mapping of the collected monitoring data itself. This paper presents an approach to monitor and evaluate the microstructure of a Laser Beam Melting (LBM) printed component. It aims to estimate the quality of the component by determining printing anomalies within the solid structure, using the fuzzy set theory for feature engineering. The anomaly detection exploits the collected melt pool data generated by image analysis with photodiode signals of microsections for the fuzzy based anomaly detection. The proposed concept is proven with nested printing anomalies.

Keywords

Additive Manufacturing · Laser Beam Melting · Process Monitoring · QM-Meltpool 3D · Uncertainty Analysis · Fuzzy · Anomaly Detection · Feature Engineering

1. Introduction

High-performance industries such as the medical, automotive and aerospace industry are in demand of a manufacturing process with a high product quality and process robustness. AM, within this work more precisely speaking LBM, as one of few manufacturing processes allows the production of high-performance component designs. However, the quality variability and a lack of quality assurance of AM manufactured components prevents the industrial breakthrough. An assured quality estimation of AM components delays the necessary verification these high-performance industries are in need for and is the key motivation for process monitoring systems. The main goal lies within the in situ detection of anomalies in the microstructure of the printed component to reliably evaluate the printing quality. Monitoring systems with photodiodes and cameras [1] are able to collect physical characteristics of the melt pool. This information is the foundation for a successful quality evaluation, as there is a correlation between melt pool data and mechanical properties [2].

1 Technische Universität Dresden, Chair of Machine Tools Development and Adaptive Controls
2 Fraunhofer Institute for Machine Tools and Forming Technology (IWU) Dresden

Nevertheless, the challenging condition of the printing process aggravates a straightforward evaluation of the melt pool data. Influences, such as the impacting laser energy density, positioning, thermal history, grain structure and the impact of by-products have a considerable effect on the microstructure and thus the mechanical properties of the printed components [3] but are hard to deterministically quantify. Especially the re-melting of already printed layers skews the collected melt pool data. All these uncertainties are undeniably influencing the printing process and therefore they have to be considered in the microstructure anomaly detection.

Within this work the main focus lies on the fuzzy based anomaly analysis of the melt pool data from a Concept Laser M2 - BJ2009 [4] printer using the LBM, LaserCUSING®, method. The material used is an AlSi10Mg (CL31AL) alloy.

2. Melt Pool Monitoring System in Laser Beam Melting

LBM is a metal 3D printing technology mainly used for prototyping and small series production. The transition to series production as well as the increasing importance of LBM in various industrial sectors [1] requires new methods for process and part quality assurance. The vast majority of monitoring systems is based on a thermal energy source although the monitoring techniques and sensors vary [5].

2.1 Concept Laser - QM Meltpool 3D

The Katholieke Universiteit Leuven developed in cooperation with Concept Laser GmbH an optical measurement system able to collect in situ thermal radiation emitted by the melting metal powder [6]. This position-related, real-time monitoring system is exclusively licenced by Concept Laser and called QM Meltpool 3D. Fig. 1 shows simplified the basic principle and appendant hardware. The key parts of the monitoring system are the infrared high-speed camera and the photodiode which are installed coaxial in the optical path between the laser source and the scanning system allowing the on axis detection of the reflecting melt pool emissions [1]. Thereby, the photodiode measures the intensity of the emitted radiation and the camera measures the area of the melt pool. By this means, it is crucial mentioning that these values are not absolute values and are only an indication of the melt pool parameters.

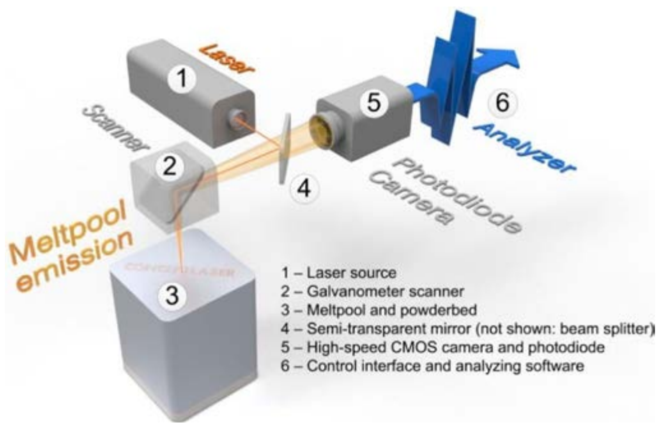

Fig. 1 Main set up of QM Meltpool 3D system [1]

Nevertheless, they are a good indicator for the melt pool stability and quality [7]. Both sensors, photodiode and camera, are capturing with a resolution up to 35 µm and a sampling rate of 50 kHz (photodiode) and 15 kHz (camera) [1].

Within this work only the data of the melt pool area by the camera system is used for the anomaly analysis, as the data recording of the melt pool intensity is less robust and prone to set up variations and process by-products [7].

2.2 Interpretation and Evaluation of QM Meltpool Data

Monitoring the melt pool area during the printing process allows a layer based analysis of variations in the melt pool dimensions. These variations are a result of various process and material influences such as an uneven powder layer deposition, grain structure irregularities within the powder, process by-products like spatter affecting the laser energy, irregular heat transfer due to the geometry of the component and more. All these external disturbances have an undeniable influence on the resulting melt pool area but are not measurable or clearly predictable. The complete printing process is guided by uncertainties, which are manifested in the melt pool area [5]. Therefore, the melt pool area data is a viable parameter for analyzing the quality of the component´s microstructure.

One crucial quality feature in LBM is the porosity, which correlates directly with the mechanical properties of the printed component, such as tensile strength and young's modulus [8]. The main challenge with this quality feature is the determination of pores within the solid structure. Post construction analysis such as computed tomography (CT) scans and the metallographic method are helpful tools to determine pores within the microstructure. Nonetheless, they do not qualify as a standardized evaluation system for LBM printed parts as they either destroy the analysing component or are strictly too expensive and elaborate to be adapted in a mass production aspired additive manufacturing process – a process monitoring evaluation QM Meltpool 3D bypasses these issues. The opportunity to predict possible pores directly from the collected melt pool data enables a mechanical quality evaluation directly out of the printer. Laser power, scan velocity, layer thickness and hatch distance determine first-hand the laser energy density [2] and are the main influence on the melt pool data. In [2] it is proven that both, insufficient or too high laser energy result in pores leading to poor component quality. Therefore, conspicuous deviations within the melt pool data might be an indicator for a poorer fused microstructure and thus worse mechanical properties. These deviations are traceable anomalies.

Regardless the interpretation of the melt pool data, one undeniable influence skews the collected melt pool data. Due to the thin layer thickness and the high laser energy density impact on the metallic powder, a re-melting of the previous, already solidified layers occurs [9]. This effect supports the attachment of metallic particles along the vertical axis and is thus crucial for a homogeneous microstructure [9]. However, it invalidates the collected melt pool data of the previous layers, as it is not in line with the current state of reality. Especially, when the re-melting effects multiple layers, re-melting the same layer numerous times, the truthfulness of the melt pool data has to be strongly questioned. The exact depth of the re-melting is difficult to quantify in an exact layer count as it depends on the laser energy, layer thickness and the material itself [9]. Therefore, an uncertain perspective on the collected melt pool data has to be applied.

3. Fuzzy Uncertainty

When referring to data uncertainty the implication is towards the uncertainty within the input data itself [10]. This is the case when for instance the presented data is distorted by measurement inaccuracies, parameter variations, arbitrary fluctuations, a lack of information or known but hard to quantify influences. All these uncertainties have an undeniable influence on the objective. Mapping these uncertain datasets on a strict probability distribution with a single probability specification does not portray the level of uncertainty that distorted and sparse data requires. In contrast to the probability model, the possibility model fuzzy logic [11] is able to grasp ill-posed [12] data with a weighted interval specification.

Most commonly uncertain data is represented by fuzzy triangular numbers [10] which is described as $\tilde{A} = < a,b,c >$, $a,b,c \in R$. As Fig 2 (a) depicts, a and c are the bounds of the lowermost interval representing the necessary range to describe the uncertain data in its entirety. Since the uncertainty is at its highest point for this interval, the degree of expectation represented by corresponding alpha-level is at its lowest, namely $\alpha_0 = 0$. The highest degree of expectation is reached at b as the value, which is most possible to be true. Between these two extrema any alpha-level $\alpha_k \in [0,1]$ identifies as a degree of expectation expressing the possibility that an event takes places within the corresponding interval. For the existing melt pool data, a fuzzy triangular number [11] is particularly suitable to describe the presented level of uncertainty. The lowest alpha-level entails the range, also known as the supper of the fuzzy number [10], and the value b describing the most possible representative of the measured data. The smaller the support, the higher the precision of the fuzzy number.

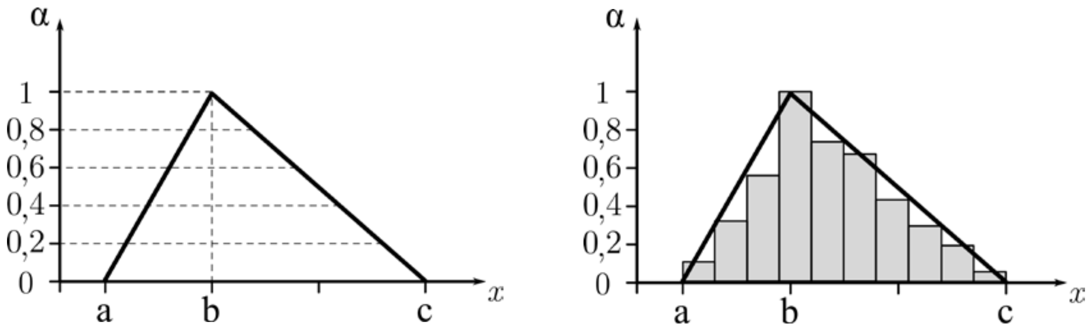

Fig.2 (a) Schematic representation of a fuzzy triangular number $\tilde{A} = < a,b,c >$,
(b) Fuzzification of a dataset via a histogram

The process of determining a suitable fuzzy number to a given data set is known as fuzzification [10]. The exact procedure often depends on the specific problem to be solved itself and bears a subjective evaluation [10]. However, a universal and objective orientated approach can be achieved with the usage of histograms. They give a sense of the underlying density distribution of the data set allowing a general evaluation of the possibility of each bin or value within the data set. Fig. 2 (b) demonstrates this correlation.

4. Anomaly Detection Algorithm

As described in Section 2.4 several sources induce a fluctuation to the printing process. For example insufficient and too high laser energy can lead to porosity. Although pores are well-known errors, this is only one possible incident that might affect the component.

Classification algorithms can directly predict the occurrence of certain errors. However, these faults have to be previously known to the algorithm. In order that such a supervised machine learning method is able to learn a function to map the data to errors or normal print results an adequate number of instances of all cases is required. Neither are all possible errors known nor exists a sufficient data set to train such classification models.

Many monitoring systems use unsupervised machine learning methods like k-means clustering. These algorithms try to divide the input data in a certain number of groups. This number often has to be set by the user before applying the algorithm. Hence, the user has to know whether and how many abnormalities occurred since a false number of groups can cause misinterpretations.

Anomaly detection systems eliminate these drawbacks. The precise error can be unknown during the training of the algorithm. However, the knowledge of good print processes is used to learn the regular behaviour. Anomalies are instances identified by the distance between the normal data points and the new abnormal data point. By this, the number of possible errors is unimportant for the system. Since the system detects not only errors but also irregularities, which might not affect the quality of the printing, abnormalities are referred to as anomalies. Pores are typical example for such an anomaly. They emerge from unusual variations of the melt pool. However, a single melting point does not lead to a pore or any other printing error due to the re-melting through neighbouring points. Therefore, single points are not treated as anomalies. In the sense of [13] a collection of related data instances should be identified as a collective anomaly. Therefore, the anomaly detection system requires a pre-processing step that converts collective anomalies to point anomalies by also taking care of the uncertainties.

4.1 Voxel Generation and Feature Engineering

The melt pool data underlies two major uncertainties – the current state of the melt pool area compared to the collected data by the QM Meltpool 3D system and the exact depth of the re-melting process (Chap. 2.2). The presented approach comprises both in different ways. First, the uncertain re-melting depth is embedded in the three-dimensional voxel geometry and the grid they are generated in. Each voxel forms a close to cubical volume element with an edge length oriented on the sum of the included layers' thicknesses. Thereby, each voxel contains the partial data of six layers. Fig. 3 (a) portrays a single three-dimensional voxel with its allocated melt pool points. Noticeable are the orthogonal aligned scan directions of two overlying, parallel scan tracks. The grid is constructed along the normalized horizontal axis so that the voxels are positioned directly next to each other, as Fig. 3 (b), showing the melt pool points of a single specimen's layer, points out. In contrast, along the vertical axis the voxels are stacked into each other in such a way that each voxel shares half of its layer count with the upper and lower positioned voxel. Although this structure leads to data redundancies, it preserves the re-melting influence of each layer onto the underlying ones. The second existing uncertainty, the distorted melt pool data, is handled with by assigning a fuzzy triangular number to each voxel based on its allocated melt pool data. Fig. 4 (a) shows the histogram of a voxel's melt pool data (green) and the corresponding generated fuzzy triangular number (red).

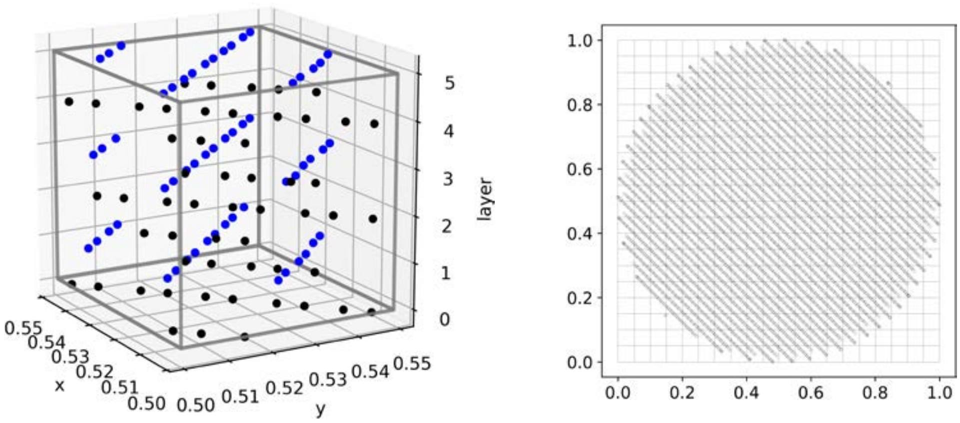

Fig. 3 (a) schematic representation of a voxel and the correspondingly allocated melt pool data (b) schematic representation of 2D voxel grid and melt pool data of a single slice

The created fuzzy number provides the basis for the anomaly detection. Thereby, to each triangular fuzzy number five characteristic features are allocatable. Fig. 4 (b) shows schematically these features as specific attributes of the fuzzy triangular number and represent different uncertainty characteristics. $\alpha_{0,min}$ and $\alpha_{0,max}$ embodies the lower and upper bound of the data set and thus the lowest and highest measured value in the voxel. The absolute interval span $\alpha_{\Delta 0}$ describes the level of precision of the voxel data. α_1 represents the value with the highest degree of expectation whereas $\alpha_{centroid}$ stands for the weighted average of the fuzzy number.

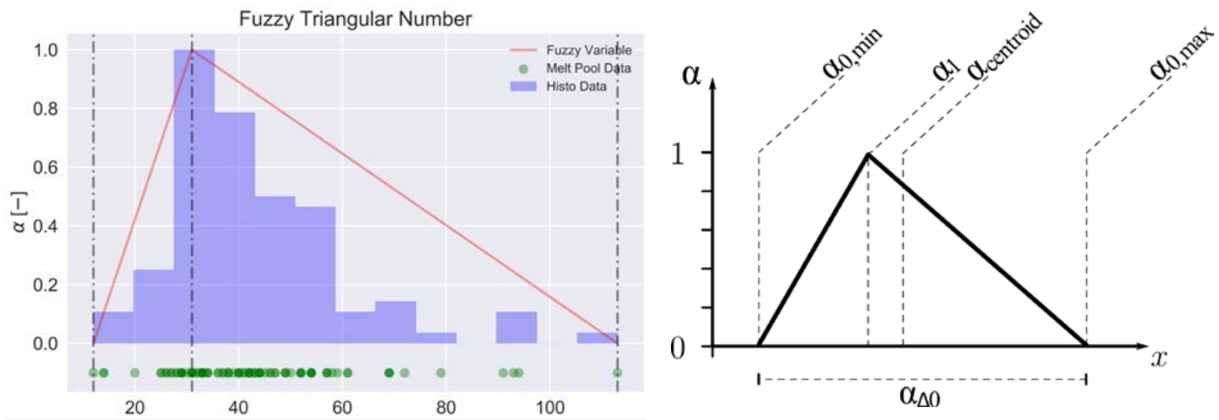

Fig. 4 (a) Generated fuzzy triangular number based on a single voxel's melt pool data (b) schematic representation of the feature set embedded in a fuzzy triangular number

4.2 Anomaly Detection (Isolated Forrest)

The isolation forest is an unsupervised machine learning algorithm feasible to identify previously unknown anomalies in a data set. In contrast to many other anomaly detection algorithms, no density or distribution from the data has to be estimated. Additionally, this method can cope with high-dimensional data sets as well as no prior knowledge of anomalies. Hence, the isolation forest is best suitable for the application to the current problem confirmed by empirical evidence that it outperforms various machine learning algorithms for anomaly detection [14].

The key idea of the isolation forest is that there are only a few anomalies, which differ from normal samples, and therefore can easily be segregated, see Fig. 5. For this purpose, the algorithm generates multiple random trees, which partition the feature space until all instances are isolated. For normal samples a single random tree requires more partitions and hence a longer branch length to fully segregate it from the remaining data. Whereas for anomalies the branches are noticeable shorter [15]. Finally, an anomaly score is calculated based on the average branch lengths.

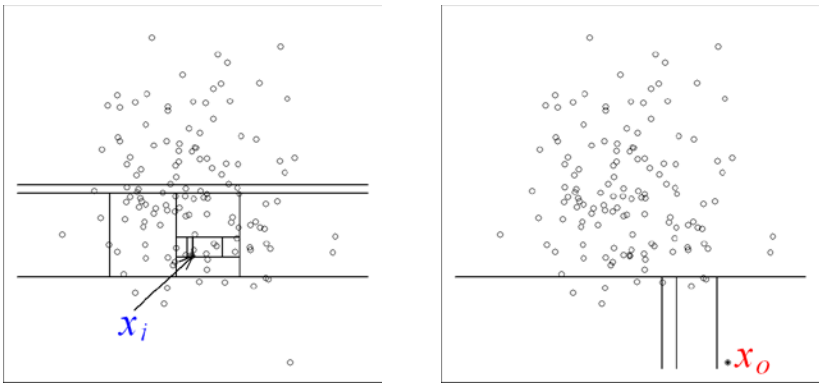

Fig. 5 Identification of normal data point vs. anomaly [5]

4.3 Detecting anomalies in specimen: strategy and verification

The overall strategy to determine possible anomalies is by training the isolated forest with the introduced feature set from Chap. 4.1 of well-constructed specimens and use this data as reference for newly printed components. This way, every conspicuousness within the new data sets will be detected and approximately located within component.

To verify the proposed method components with build-in errors are analyzed. The error batch resolves around a layer based anomaly, where the default machine settings are purposefully set up to aggravate the microstructural density and thus force the creation of pores. Thereby the specimens are printed with default settings (Tab. 1), except for a sum of sequential layers. These layers vary from the default settings in only one particular input variable. As is shown in [2] all four laser energy parameters have a significant influence on the porosity and vary in their sensitivity depending on the resulting laser energy. For this analysis laser power and hatch distance were changed. Overall, three different variations from the default settings are implemented: a bisection of the hatch distance, a doubling of the hatch distance and a down setting of the laser power. Tab. 1 lists the default settings and the three implemented error variations.

Tab. 1 Identification of normal data point vs. anomaly

parameters	default settings	error layer #1	error layer #2	error layer #3
laser power [W]	370	370	370	*270*
scan velocity [mm/s]	1400	1400	1400	1400
layer thickness [mm]	0,05	0,05	0,05	0,05
hatch distance [mm]	0,112	*0,056*	*0,224*	0,112

5. Results

As the anomaly detection is based on a machine learning algorithm the data is split into a training, a validation and a test set. This procedure is necessary to prevent an overfitting to the current problem and ensures the generalizability of the solution. The isolation forest and the computation of the anomaly score is learned by the train set which stems from three specimens disassembled into about 168000 voxels showing no known anomalies. The validation set contains about 546000 voxels from four specimens which have one of the presented three error layers. Thus about 4% of all voxels, namely about 24000, are potential anomalies. This data is used to tune the hyperparameters of the isolation forest, to specify the threshold for the anomaly score identifying abnormal voxels and to evaluate the performance of the approach. The final test is conducted with specimens containing three error layers as described in Tab. 1, see also Fig. 6. The performance of the monitoring system is evaluated by the identification of the modified layers. The percentage of the detected anomalies in the regular and the modified regions provide an additional measure for the robustness and sensitivity.

5.1 Implementation Details

In the data preparation smaller voxel sizes have been evaluated, however, the chosen size of six layers per voxel performed significantly better. For the implementation of the anomaly detection system various hyperparameters have been tested using a grid search. This includes the number of trees ranging from 400 to 1000, the percentage of the training data used for each estimator ranging from 0.5 to 1.0, the number of features for each estimator ranging from 1 to 5 and finally the threshold in order to decide whether the calculated anomaly score results in an anomaly or not ranging from 0.03 to -0.19. The optimization of the hyperparameters was conducted on a separate data set. Hence, the anomaly detection system has not seen the final test data before.

5.2 Experimental Results

Fig. 6 shows one test specimen with three error layers according to Tab. 1, in particular on the left, the model displaying the modified layers in red. Second to left, the printed specimen obviously reveals the error layer #2 in the middle; below that the error layer #1 is also recognizable; the error layer #3 in the upper part is hardly visible. The next graphics on the right illustrate the anomaly score from the isolation forest and the detected anomalies.

The anomaly detection accomplished the best identification rate for the error layer #1, which was printed with half of the default hatch distance. The dense melting points yield to more points for the voxel generation improving the precision level of the fuzzy number. Hence the algorithm achieves a detection rate of almost 88 %. Consequently this error layer #1 is easily identified in contrast to the error layer #2 which was printed with a doubled hatch distance. This kind of error is rather unusual in current printing processes. Containing fewer melting points per voxel, the uncertainty increases and complicates the anomaly detection for the isolation forest. Nevertheless, even the low rate of detection, 4 %, indicates that this region should be checked by the operator. This rate is sufficient compared to a rate of detection of at most 0.53 % for the normal regions which originates from the boundary points as Fig. 6 shows. Most importantly, the approach clearly identifies error layer #3 as anomalies by a rate of detection of about 47 %. The lower laser power presents a non-visible modification of the specimen. As a low energy input affects the re-melting and hence the bond of successive printing layers this kind of error is crucial for the strength of the specimen. Thus, an anomaly detection during the printing process can identified undesired weaknesses.

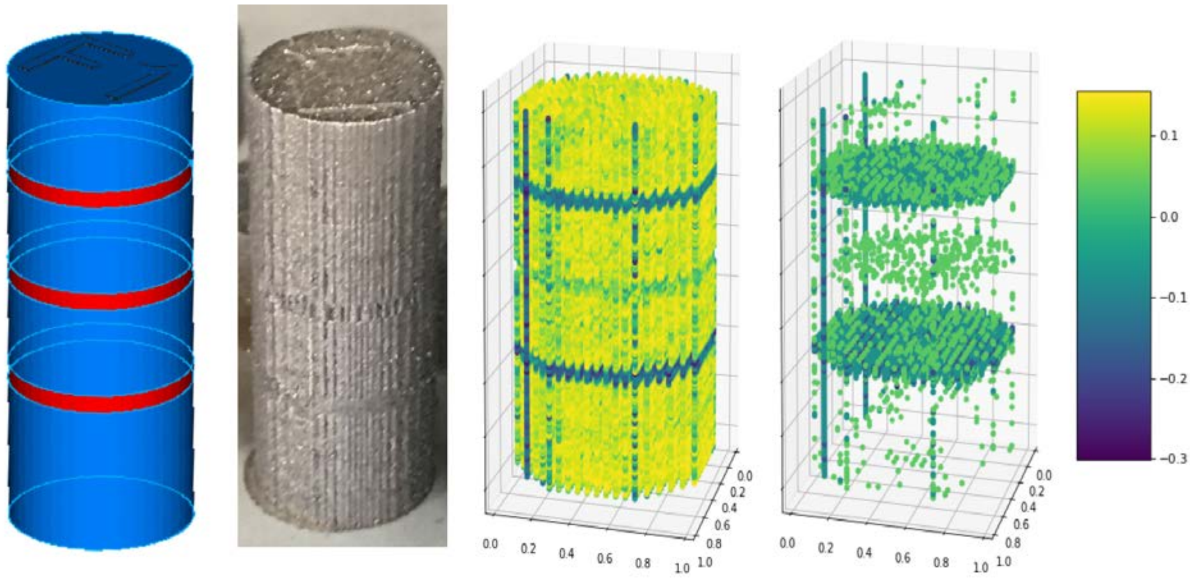

Fig. 6 Validation specimen with build in error layers (model, real specimen and anomaly score plots)

6. Evaluation

The resulting outcome verifies the functionality of the proposed fuzzy based anomaly detection. The implanted error layers were identified successfully, although not every error type at the same success rate. Enlarging the hatch distance seemed to be less conspicuous for the anomaly detection as downsizing the hatch distance or decreasing the laser power, up to the point that it is not noticed as a high-level anomaly. However, looking at the standard application of LBM manufacturing processes, this observation does not effect the proposed method, as the hatch distance is a rather certain setting whereas fluctuations in the arriving laser energy density due to manufacturing-related laser power uncertainties and thus potential errors are more common.

Future enhancements, such as an enriched, component-geometry adapted voxel grid structure, can improve the detection of anomalies. Noticeable are the anomaly boundary points, which on the one hand might appear due to the current grid structure or on the other due to the one sided laser energy exposure of the powder and thus a weaker binding. In addition to that, further processing of the detected anomalies with pooling or clustering algorithms may lead to a clearer recognition of irregularities. Furthermore, the current learning data set is not examined for flaws in the microstructure, for instance with CT scans, and thus might lead to less sensitive detections. The purification of the learning data is a crucial step to improve the anomaly detection.

All in all the proposed method leads to promising results and is able to be used as a real-time in situ process monitoring algorithm, which works independent of the components geometry parameters and improves overtime, as the learning data grows and purifies with every print.

Acknowledgement

Parts of this research were funded by the German Federal Ministry of Education and Research, grant number 03ZZ0212G “Zwanzig20 - Agent-3D - Verbundvorhaben: QUALIPRO”.

References

[1] T. Toeppel, P. Schumann, M. Ebert, T. Bokkes, K. Funke, M. Werner, F. Zeulner, F. Bechmann and F. Herzog: 3D analysis in laser beam melting based on real-time process monitoring, Proceedings, Materials Science and Technology Conference, Salt Lake City (2016), pp. 23-27

[2] C. Rosenkranz, S. Schmid, M. Lutter-Günther, C. Seidel and G. Reinhart: Investigation of the correlation between signal characteristics of photodiode-based melt pool monitoring and part quality in laser-based powder bed fusion of AlSi10Mg, Proceedings, MAMC, Wien (2018), pp. 51-62

[3] O. Rehme: Cellular design for laser freeform fabrication, (Ph.D. thesis, Technische Universität Hamburg-Harburg, Germany, 2009)

[4] N.N.: Neue Möglichkeiten mit 3D (New possibilities in 3D), Werkzeug & Formenbau, (2015, Volume 9-4), pp. 64-66

[5] G. Tapia and A. Elwany: A review on process monitoring and control in metal-based additive manufacturing, Journal of Manufacturing Science and Engineering (2014, Volume 136-6), pp. 60801-1-60801-10

[6] T. Craeghs, S. Clijsters, J. Kruth, F. Bechmann and M. Ebert: Detection of process failures in layerwise laser melting with optical process monitoring, Physics Procedia (2012, Volume 39), pp. 753 – 759

[7] S. K. Everton, M. Hirsch, P. Stravroulakis, R. K. Leach and A. T. Clare: Review of in-situ process monitoring and in-situ metrology for metal additive manufacturing, Materials and Design (2016, Volume 95), pp. 431–445

[8] A. B. Spierings, M. Schneider and R. Eggenberger: Comparison of density measurement techniques for additive manufactured metallic parts, Rapid Prototyping Journal (2011, Volume 17-5), pp. 380–386

[9] J. Trapp, A. M. Rubenchik, G. Guss and M. J. Matthews: In situ absorptivity measurements of metallic powders during laser powder-bed fusion additive manufacturing, Applied Materials Today (2017, Volume 9) pp. 341–349

[10] B. Möller, W. Graf and M. Beer: Fuzzy structural analysis using α-level optimization, Computational Mechanics (2000, Volume 26), pp. 547-565

[11] T. J. Ross: Fuzzy Logic with engineering Applications, Wiley, New York, 2010

[12] V. N. Vapnik: The nature of statistical learning theory, Springer, New York, 1999

[13] V. Chandola, A. Banerjee and V. Kumar: Anomaly detection: a survey, ACM Computing Surveys (2009, Volume 41-3), pp. 15:1-15:58

[14] F. T. Liu, K. M. Ting and Z. Zhou: Isolation-based anomaly detection, ACM Transactions on Knowledge Discovery from Data (2012, Volume 6-1), pp. 3:1-3:39

[15] F. T. Liu, K. M. Ting and Z. Zhou: isolation forest, Proceedings, 8th IEEE International Conference on Data Mining, Pisa, 2008, pp. 413-422